Wave propagation in a one-dimensional quasiperiodic medium: Localization and intermittency

J. Peyraud and J. Coste
Laboratoire de Physique de la Matière Condensée, Université de Nice, Parc Valrose, 06034 Nice Cédex, France
(Received 29 June 1987)

We consider the propagation of a wave in a quasiperiodic medium whose refractive index exhibits δ-like peaks of equal amplitudes and which are located on quasiperiodic sites. Two specific models of site distributions are investigated. In the first one, we find "quasilocalized states" with a very critical definition in energy. In the second model, a particular type of intermittency and a phenomenon of "noise localization" appear. The properties of the two models are based on the existence of a slow variable for particular energy values. Experimental applications of the observed resonances are suggested.

INTRODUCTION

We study here the propagation of a classical wave (acoustic or electromagnetic) in a one-dimensional medium whose refractive index $\nu(x)$ exhibits a set of δ-like peaks with equal amplitudes and located on quasiperiodic sites. This problem is mathematically equivalent to solving a Schrödinger equation where the potential is proportional to $\nu(x)$. A complementary class of problems has already been investigated, namely those in which the potential peaks are regularly spaced with quasiperiodic amplitudes (an extensive review is to be found in Sokoloff's paper[1]).

We show that interesting things happen, noticeably localization, when the phase shifts experienced by the wave in successive interpeaks intervals can be characterized by a slow variable; and this situation occurs at definite values of the energy (or wave frequency).

Our method will consist of studying the dynamics of the phase shift between forward and backward waves. We are thus led to iterate a non autonomous mapping on the circle. One of the advantages of this method is that it permits a simple and clear cut distinction between a localized and a stop-band state. We show that localization takes place in the pass bands, or equivalently is associated with irrational rotation numbers of the circle map. Actually our solutions are not L^2 integrable, and therefore not localized in the conventional sense. But they contain a vanishing stored energy by unit length; moreover some of them exhibit no recurrent behavior. We call these solutions "quasilocalized."

In the first part of this paper we define the two particular $\nu(x)$ fields which will be studied, and we call A and B the associated models. Then we derive the above mentioned angular mapping, and give some general properties concerning the eigenvalue problem and the rotation numbers. Finally we study separately models A and B, whose properties are substantially different. In model A localized states are obtained, with one or several peaks and a very critical definition in energy. In model B we describe a particular type of intermittency, and the phenomena of noise localization and antilocalization.

The models: General properties

We consider a one-dimensional medium whose refractive index is uniform, except on a countable set of sites ("barriers") where identical δ-like variations takes place. The barriers are distributed almost periodically according to specific laws which will be given below. Each such variation can be described (Fig. 1) as the limit of a finite domain of width a and wave number k, when $k/k_0 \to \infty$ and $ka \to 0, \varepsilon$ being finite and arbitrary. The frontier abcissas x_n are distributed almost periodically according to specific laws which will be given below. Such a field of refractive indexes reads $\nu(x) = \varepsilon \sum_n \delta(x - x_n)$.

Let $Y_+ e^{ikx}$ and $Y_- e^{-ikx}$ be the amplitudes of forward and backward waves (Fig. 2). Writing the continuity of the field and its derivative through a barrier imposes a matricial relation between the 2-vectors $\mathbf{Y} = \{Y^+, Y^-\}$ and $\mathbf{Y}'$ on each side of the barrier: $\mathbf{Y}' = T\mathbf{Y}$, where

$$T = \begin{bmatrix} 1+i\varepsilon & +i\varepsilon \\ -i\varepsilon & 1-i\varepsilon \end{bmatrix}.$$

It can be shown that a transfer matrix of the above form is also a good approximation for a barrier of finite width provided k/k_0 is close to unity and the phase shift through the barrier is small. Transfer matrices of this form are also found in the propagation of a surface acous-

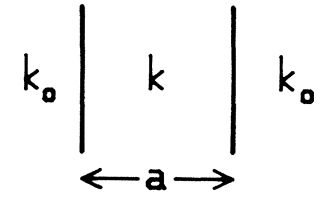

FIG. 1. Representation of a barrier.

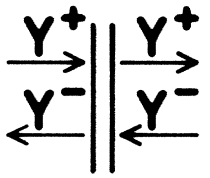

FIG. 2. Inward and forward amplitudes around a barrier.

tic wave on a grooved array.[2]

Let us now define the transfer matrix which relates amplitude vectors $\mathbf{Y}_j$ and $\mathbf{Y}_{j+1}$ on the left of two successive barriers (Fig. 3):

$$\mathbf{Y}_{j+1}=A_j\mathbf{Y}_j \tag{1}$$

where

$$A_j=\begin{bmatrix} e^{i\phi_j} & 0 \\ 0 & e^{i\phi_j} \end{bmatrix}\cdot T=\begin{bmatrix} \alpha_j & \beta_j \\ \beta_j^* & \alpha_j^* \end{bmatrix}, \tag{2}$$

$\phi_j=k_0 l_j$ being the phase shift experienced by the wave along interval l_j,

$$\alpha_j=e^{i\phi_j}(1+i\varepsilon),\text{and } \beta_j=i\varepsilon e^{i\phi_j} . \tag{3}$$

Let us now introduce $U_j=Y_j^+ + Y_j^-$, which is the total wave's amplitude at the jth frontier. From relation (1) we deduce the following real recurrence relation obeyed by U_j:

$$U_{j+1}/\sin\phi_j + U_{j-1}/\sin\phi_{j-1} - [\sin(\phi_j+\phi_{j-1})/(\sin\phi_j\sin\phi_{j-1}-2\varepsilon]U_j=0 . \tag{4}$$

As could be expected, this relation has the same form as those obeyed by a solution of a stationary Schrödinger equation containing a potential $V(x)=v(x)$ (and with $\phi_n=x_n-x_{n-1}$). This relation may be found for instance in Sokoloff's review paper[1] [Eq. (32)]. When the δ peaks are regularly spaced ($x_n=na$) and ε is periodically dependent on n with a period incommensurate with a, the problem is reducible[3] to the Aubry and André model[4] (linear chain of atoms submitted to the action of an external potential whose period is incommensurate with interatomic distance). In our case (ε constant and ϕ_n quasiperiodic), Eq. (4) does not possess the self-duality property of corresponding equations in Aubry and André or Ostlund and Pandit[5] models. Therefore we cannot apply to our problem the argument based on self-duality and on the use of Thouless exponent—an argument which shows the existence of a localization transition for a definite value of the model parameters. We shall see below that there is good evidence for thinking that such a transition does not exist in our model.

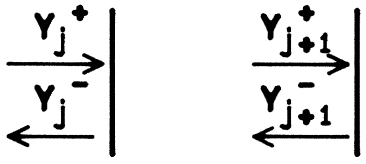

FIG. 3. Inward and forward amplitudes on the left of two successive barriers.

We shall write interpeak phase shifts in the form

$$\phi_j=(E/2)\zeta_j , \tag{5}$$

where $\zeta_j=x_{j+1}-x_j$ is the dimensionless length of the jth interval, and $E=2k_0 l$ has the meaning of the energy parameter of the equivalent Schrödinger equation, l being a characteristic length scale of our propagating medium. We shall take $l=1$ in the following. We shall now define the distribution of the x_j's (or ζ_j's) in the two models we have considered.

Model *A*

Let P and Q be two relatively prime numbers. The model is defined by the fact that the positions x_j of the barriers are any multiples of P and Q. Equivalently $v(x)$ is of the form

$$v(x)=\varepsilon\left[\sum_m \delta(x-mP)+\sum_n \delta(x-nQ)\right] . \tag{6}$$

Let us put

$$\rho=P/Q . \tag{7}$$

The set of intervals $\{\zeta_j\}$ is periodic with period $M=P+Q-1$ if ρ is rational, aperiodic in the opposite case. The only aperiodic case considered here will correspond to $\rho=\sigma=(\sqrt{5}-1)/2$ (golden mean), and the rational values of ρ will be the set of the successive approximants of σ: F_N/F_{N+1}, $\{F_N\}$ being the set of Fibonacci numbers (defined iteratively as $F_n=F_{n-1}+F_{n-2}$ for $n\geq 3$, with $F_1=1$ and $F_2=2$). For given N, the spatial period (in unit length l) is $L=PQ$ and goes to infinity when $\rho\to\sigma$.

An important property of this model is that, for ρ rational, the barriers (and therefore the intervals) are symmetrically distributed inside a period around its center $L/2$; that is, we have $v(x)=v(L-x)$. Intervals ζ_j take all integer values in $[1,P]$. Each interval appears two times (on symmetrical sites with respect to the period center), except for interval P, which is found many times [its average rate of occurrence for large N is approximately $(1-\rho)/(1+\rho)$].

Model *B*

Model B is defined by

$$\zeta_j=(\rho j)[\text{mod}(1)] . \tag{8}$$

Again ρ will be either σ or F_N/F_{N+1}. The set $\{\zeta_j\}$ contains all the multiples of $1/Q$; that is, ζ_j is of the form $m(j)/Q$ with integer $m(j)$ verifying $1\leq m(j)\leq Q-1$. If ρ is rational there are $M=P+Q-1$ intervals ζ_j and the spatial period is given by $L=(Q-1)/2$.

Transfer matrices and angular mapping

Iterating matrix relation (1) up to $j=n$, we obtain $\mathbf{Y}_n=\mathring{A}_n\mathbf{Y}_0$, where $\mathring{A}_n=\prod_{j=1}^{j=n}A_j$ and we call "orbit of $\mathbf{Y}_0$" the set $\{\mathbf{Y}_n\}$ of the successive iterates of $\mathbf{Y}_0$. In our nondissipative model, the conservation of field energy im-

poses that $\mathring{A}_n$ has the same structure as A_n, namely

$$\mathring{A}_n = \begin{bmatrix} a_n & b_n \\ b_n^* & a_n^* \end{bmatrix},$$

with $\det(\mathring{A}_n) = |a_n|^2 - |b_n|^2 = 1$. In the case of a periodic system (ρ rational), where the period contains M iterations of the above application, one may define the stop bands of the system through the eigenvalues $s_{1,2}$ of $\mathring{A}_M(E,\varepsilon)$ which are the roots of the characteristic equation $s^2 - 2\mathrm{Re}(a_M)s + 1 = 0$. These roots, whose product is equal to unity, are either real or of the form $e^{\pm i\varphi}$ [$\varphi = \arccos(\mathrm{Re}\, a_M)$].

The real range of $s_i(E,\varepsilon)$ defines in the (E,ε) plane the set of the stop bands. The eigenvector orbits are nothing but the two fundamental Floquet solutions of the problem.

Let us now turn to the angular map. We put

$$W_n = Y_n^+ / Y_n^- \tag{9}$$

and use recurrence relation (1) to obtain $W_{n+1} = e^{2i\phi_n} S_n$ with

$$S_n = [(1+i\varepsilon)W_n + i\varepsilon]/(1 - i\varepsilon - i\varepsilon W_n) .$$

We see that if $|W_0| = 1$, then $|S_0| = 1$ and $|S_n| = |W_n| = 1 \quad \forall n > 0$. Initial states verifying $|W_0| = 1$ will be said to belong to "class W" and we shall essentially study them in the following. This may seem quite restrictive. However, we observe that any initial-state vector $\mathbf{Y}$ can be projected over two independent vectors $\mathbf{u}_1, \mathbf{u}_2$ belonging to class W, and the orbit of $\mathbf{Y}$ is a linear combination of $\mathbf{u}_1$ and $\mathbf{u}_2$ orbits. We shall have to examine how the properties of a general solution can be derived from those of class-W orbits.

An equivalent angular mapping is obtained by considering the variable

$$Z_n = e^{-i\phi_{n-1}}(Y_n^+ / Y_{n-1}^+) . \tag{10}$$

Z_n obeys the following recurrence formula:

$$Z_{n+1} = 1 + i\varepsilon + e^{-2i\phi_{n-1}}(1 - i\varepsilon - 1/Z_n) . \tag{11}$$

Now putting

$$V_n = Z_n - (1+i\varepsilon) , \tag{12}$$

we see that V_{n+1} is related to former W_n by $V_{n+1} = i\varepsilon / W_n$. Therefore $|W_n| = 1$ implies $|V_n| = \varepsilon$. Assuming therefore that

$$V_n = \varepsilon e^{i\theta_n} , \tag{13}$$

we obtain the following recurrence relation obeyed by θ_n:

$$\theta_{n+1} = \theta_n - 2\phi_{n-1} - 2\beta_n , \tag{14}$$

$$\beta_n = \arctan[\varepsilon(1+\sin\theta_n)/(1+\varepsilon\cos\theta_n)] . \tag{15}$$

Relations (14) and (15) have a simple geometrical interpretation, as shown in Fig. 4. The circle (Ω,ε) is invariant under the transformation, and V_n is the image of complex number Z_n in a reference frame centered at Ω.

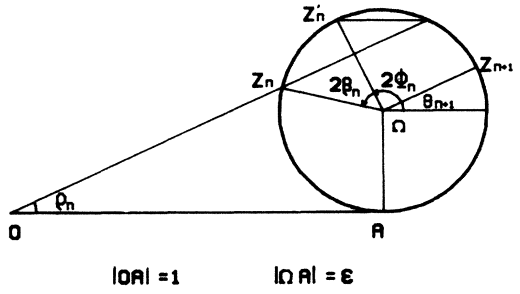

FIG. 4. Geometrical interpretation of the angular mapping.

Equations (14) and (15) define an n-dependent, nonlinear mapping on the circle which is equivalent to the original linear matrix transformation on $\mathbb{C}\otimes\mathbb{C}$. Relations (10)–(13) permit one to evaluate Y_n^+ in terms of initial value Y_0^+ and of the set of θ_j successive values:

$$Y_n^+ = Y_0^+ \prod_{j=1}^{n} e^{i\phi_{j-1}}(1 + i\varepsilon + \varepsilon e^{i\theta_j}) , \tag{16}$$

from which we obtain the expression for the wave intensity:

$$I_n = |Y_n^+|^2 + |Y_n^-|^2 = 2|Y_n^+|^2$$
$$= I_0 \prod_{j=1}^{n} [1 + 2\varepsilon\cos\theta_j + 2\varepsilon^2(1+\sin\theta_j)] . \tag{17}$$

An important property of the nonautonomous mapping on the circle is that its Jacobian is always different from zero. Indeed

$$\partial\theta_{n+1}/\partial\theta_n = [(1+\varepsilon\cos\theta_n)^2 + \varepsilon^2(1+\sin\theta_n)^2]^{-1} \neq 0 ,$$
$$\forall \varepsilon, E, \theta_n .$$

Therefore transformation $\theta_n \to \theta_{n+1}$ does not exhibit any critical point, whatever the E and ε values are. This fact constitutes a strong presumption against the existence of a localization transition.

Stop bands, $\nu(x)$ Fourier transform, and rotation numbers

In the limit $\varepsilon \to 0$, the energy spectrum of the stop bands becomes punctual, and we shall show that it is then identical to the Fourier-transform of $\nu(x)$. Indeed, in this limit, the angular mapping reduces to

$$\theta_{j+1} = \theta_j - E\zeta_{j-1} .$$

Therefore $\theta_n = -E\sum_{j=1}^{j=n}\zeta_{j-1} = -Ex_n$ (taking for simplicity $\theta_1 = 0$).

Now a Floquet state in a stop band is associated with a growth rate Γ over one period ($\Gamma = I_{n+M}/I_n$) different from unity. Let us put

$$E = 2\pi\mu/L . \tag{18}$$

Using relation (17) and the above expression for θ_n, Γ reads in the limit of small ε:

$$\Gamma = 1 + 2\varepsilon \sum_{j=1}^{M} \cos(2\pi\mu x_j / L) .$$

This expression is proportional, for integer μ, to the real part of the $\nu(x)$ Fourier transform. Therefore the stop bands in the limit $\varepsilon \to 0$ are associated to integer values of μ ($E/(2\pi) \in [0,1]$). However, some of the Fourier components may vanish. In the case of model A, Fourier components ν_s have the remarkably simple form $\nu_s \simeq Q\sum_q \delta_{s,qQ} + P\sum_p \delta_{s,pP}$ with p and q integers. Therefore $\mu = pP$ and $\mu = qQ$ are the stop-band energy values such that $(\Gamma - 1)/\varepsilon$ does not vanish in the limit $\varepsilon \to 0$. For ε small but finite, all stop bands give a nonzero $(\Gamma - 1)/\varepsilon$, while their energy is shifted by an amount proportional to ε and they acquire a finite width $\Delta\mu$ ($\Delta\mu \simeq \varepsilon$). However, numerical calculations show that the stop bands whose μ is near pP or qQ have much larger growth rates than the other ones. We call them "dominant stop bands." Therefore a remarkable property of model A is that, for $\varepsilon \to 0$, the set of dominant stop bands is identical (in μ units) to those of ν_s. Since the supports of $\nu(x)$ and ν_s are themselves identical, the property can be stated in the following way: In the limit $\varepsilon \to 0$, the energy spectrum $\{\mu_k\}$ of dominant stop bands is identical to the set $\{x_j\}$ of refractive index peaks.

A quantity is invariant inside a stop band, namely the rotation number W. It will be defined as

$$W = \lim_{n \to \infty} |\theta_n - \theta_0| / (2\pi n) \quad (\text{for } \rho = \sigma) . \tag{19}$$

When ρ is rational and E belongs to a stop band, any state vector Y_0 can be decomposed over the two eigenvectors of $\mathring{A}_M$; therefore its orbit can be written as the sum of two Floquet solutions in the form

$$Y_{kM+n} = as^{kM} F_M(n) + bs^{-kM} G_m(n) \quad (\rho \text{ rational}) , \tag{20}$$

s and s^{-1} being the Floquet exponents (i.e., the $\mathring{A}_M$ eigenvalues), F_M and G_M being periodic functions of period M. Asymptotically (k large) the second term in the above expression goes to zero and we get

$$Z_{kM+n} \to e^{-i\phi_{n-1}} F_M^+(n)/F_M^-(n-1) ,$$

which is a periodic function of n with period M. Therefore the asymptotic orbit of any initial point in the angular mapping is itself periodic and contains M points. Then W may be written as

$$W = \lim_{n \to \infty} |\theta_{n+M} - \theta_n| / (2\pi M) .$$

In the limit $\varepsilon \to 0$, we have seen that $|\theta_{n+M} - \theta_n| = 2\pi\mu x_M / L$, where $x_M = L$. Therefore $W(E, \varepsilon \to 0) = \mu/M = E/(2\pi)$. As was expected, rational values of W are associated to the stop bands, and two neighboring stop bands correspond to rotation numbers differing by $1/M$. These properties survive for finite ε.

MODEL A

Symmetry, pass bands, and localization

The following considerations have only a qualitative interest and are given in order to provide a physical intuition of the phenomena. Roughly speaking, a localized state is such that its energy is localized around one or several peaks inside the system. On the contrary, the energy of a state in a stop band is essentially concentrated near one of the boundaries (exponential behavior of the orbits). In the following (unless differently stated), we shall consider a "system" (propagative medium) which contains one period L of $\nu(x)$.

Now an important property of model A is the symmetry of refractive-index field with respect to the period center $L/2$. As a consequence, the orbits $\Lambda_{1,2}(x)$ of the two eigenvectors in a pass band [associated to imaginary eigenvalues of $\mathring{A}_M(E,\varepsilon)$] have the same norm, which is symmetric with respect to $L/2$:

$$\|\Lambda_1(x)\| = \|\Lambda_2(x)\| = \|\Lambda_i(x - L)\|$$

(see Appendix A). Let us call H_{tot} and H_{left}, respectively, the entire system and left half-system. Generically, the stop bands of H_{tot} do not coincide with those of H_{left}. Therefore the pass bands of H_{tot} and the stop bands of H_{left} generally overlap. For large N some pass bands become vanishingly small (as we shall see), making this overlapping highly efficient. Figure 5 shows a numerical example where a narrow pass band of H_{tot} is immersed into a large stop band of H_{left}.

Let us choose an energy value falling in a pass band of H_{tot} and in a stop band of H_{left} and consider an eigenvector $\mathbf{u}$ of H_{tot}. $\mathbf{u}$ can be projected over eigenvectors $\mathbf{v}_1, \mathbf{v}_2$ of H_1; its orbit Λ will be a linear combination of the orbits $\mathbf{V}_1$ and $\mathbf{V}_2$ of $\mathbf{v}_1$ and $\mathbf{v}_2$. Assume now that the eigenvalue associated with $\mathbf{v}_1$ is very large and the norm of $\mathbf{V}_1$ is concentrated near $L/2$ (this actually happens: see below). Then Λ is very close to $\mathbf{V}_1$, and, due to the sym-

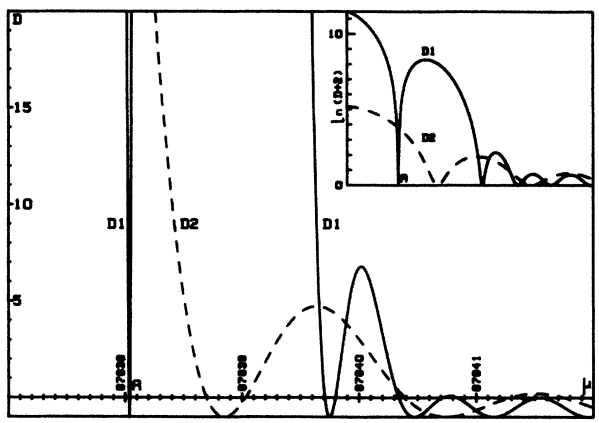

FIG. 5. Stop bands of H_{left} and H_{tot}. They are characterized by the discriminant $D(\mu,\varepsilon)$ of the eigenvalue equation of $\mathring{A}_M(\mu,\varepsilon)$ ($D = [\text{Re}(a_M)]^2 - 1$), $-1 \le D \le 0$ inside a pass band, $D > 0$ inside a stop band. D_2 and D_1 are respectively associated with H_{left} and H_{tot}. The smallest pass band of H_{tot} (later called "fundamental pass band") is located around $\mu = 67\,838.038$: point A of the graphics. It is so narrow ($\Delta\mu = 0.0078$) that it almost reduces to a vertical line around point A. A is located inside a large stop band of H_{left}. As expected, aside from the large stop bands surrounding A, the spacing of secondary stop bands of H_{left} is twice those associated with H_{tot}. The numerical parameter values are $N = 13$ and $\varepsilon = 0.01$.

metry of $\|\Lambda\|$ around $x=L/2$, we expect that Λ is peaked around this point and therefore localized.

This argument leads us to look for localized states in small pass bands, surrounded by dominant stop bands. It also emphasizes the role played by symmetry in the localization process.

The fundamental localization

According to the preceding considerations let us look for small pass bands. We have shown that, in the limit $\varepsilon\to 0$, the set of dominant stop band (SB) energies is the same as the set $\{x_j\}$ of barriers positions. Therefore the set of energy intervals between dominant stop bands is the same as the set $\{\zeta_j\}$ of interpeaks intervals. Now the two smallest ζ_j intervals are equal to unity and they are located symmetrically with respect to the period center. For a given value N of the Fibonacci-approximant ($\rho_N=F_N/F_{N+1}$), they correspond, respectively, to μ intervals $[F_{N+1}F_{N-2},F_NF_{N-1}]$ ($E\approx\sigma^2$) and $[F_N^2,F_NF_{N+1}]$ ($E\approx\sigma$). We call these energy bands the fundamental pass bands. We shall consider the first one, and put $\mu_1^0=F_NF_{N-1}$ and $\mu_2^0=F_{N+1}F_{N-2}$. We have

$$\Delta\mu^0=\mu_2^0-\mu_1^0=F_{N+1}F_{N-2}-F_NF_{N-1}=(-1)^N \qquad (21)$$

(superscript "0" refers to the limit $\varepsilon\to 0$). The above recursion relation between the F_j's follows from a well-known property of the Fibonacci numbers, namely that two consecutive approximants of σ, F_N/F_{N+1} and F_{N-1}/F_N, are "Farey neighbors" (that is $|F_{N+1}F_{N-1}-F_N^2|=1$). Expression (21) is an immediate consequence of the fundamental relation $F_N=F_{N-1}+F_{N-2}$, defining the Fibonacci numbers. Remark that $\Delta\mu^0/\mu_1^0$ goes to 0 as σ^N for large N. The above fundamental pass band is delimited by ε-independent rotation numbers $W_1=F_{N-1}F_N/M$, $W_2=F_{N+1}F_{N-2}/M$, whose distance is $\Delta W=1/M$. For small enough ε ($\varepsilon<1/F_N$), pass band $[W_1,W_2]$ corresponds to $\mu\in[\mu_1^0,\mu_2^0]$. This is no longer true for $\varepsilon\gg 1/F_N$.

We now came to the slow variable entering the problem. A preliminary observation, specific to model A, is that the ordered sequence of ζ_n intervals contains two types of subsequences, called sequences (1) and (2). Their structures are, respectively,

sequence(1): $P, m_j, P-m_j, Q-P+m_j, 2P-Q-m_j$;

sequence(2): $P, m_k, P-m_k$,

where m_j and m_k are integers such that

$$1\le m_j<2P-Q\le m_k<Q-P \ . \qquad (22)$$

Sequences alternate according to the following rules: (i) (2) is necessarily followed by {1}, and (ii) (1) may be following either by (1) or by (2) but there are at most two successive (1) sequences. Therefore a typical $\{\zeta_n\}$ sequence will be of the form

$$(1)(2)(1)(1)(2)(1)(2)(1)(1)(2)\cdots$$

(it is exactly the type of kneading sequences observed at the critical point for period-doubling bifurcations, in the logistic map).

Let us denote $(1)_m$ [$(2)_m$] the sequence (1) [(2)], whose first interval following P is m. It is easy to determine the variation of m in the three transitions $(2)_m\to(1)_{m'}$, $(1)_m\to(1)_{m'}$, and $(1)_m\to(2)_{m'}$. Putting $\delta m=m'-m$, for transitions $(2)_m\to(1)_{m'}$, we have $\delta m=Q-2P$; for transitions $(1)_m\to(1)_{m'}$ and $(1)_m\to(2)_{m'}$, we have $\delta m=2Q-3P$. Now a set of (1),(2) sequences induces a set of intervals $m_1,m_2,\ldots$. Let α_j be the phase shift produced by interval m_j in Eq. (14): $\alpha_j=2\phi(m_j)=2\pi\mu m_j/(F_NF_{N+1})$. We shall evaluate the increments $\delta\alpha$ associated with the above δm, taking into account the fact that the α_j's must be taken mod(2π).

Let us first consider the case $\mu\in[\mu_1^0,\mu_2^0]$ (corresponding to $\varepsilon<1/F_N$). We put

$$\mu/(F_NF_{N+1})=F_{N-2}/F_N-c/(F_NF_{N+1})$$
$$=F_{N-1}/F_{N+1}+(1-c)/(F_NF_{N+1}) \ ,$$

with $0<c<1$, and assume even N.

Now transitions $(1)_m\to(1)_{m'}$, and $(1)_m\to(2)_{m'}$ give

$$\delta\alpha/(2\pi)=(2F_{N+1}-3F_N)\mu/(F_NF_{N+1})$$
$$=2F_{N+1}[F_{N-1}/F_{N+1}+(1-c)/(F_NF_{N+1})]$$
$$-3F_N[F_{N-2}/F_N-c/(F_NF_{N+1})]$$

from which, since the F_j's are integers

$$\delta\alpha=2\pi[2(1-c)/F_N+3\gamma/F_{N+1}]\ [\mathrm{mod}(2\pi)] \ . \qquad (23)$$

In the same way, one finds for transition $(1)_m\to(2)_{m'}$

$$\delta\alpha'=2\pi[(1-c)/F_N+2\gamma/F_{N+1}]\ [\mathrm{mod}(2\pi)] \ . \qquad (24)$$

From here forward α will be understood as mod(2π). We see that $\delta\alpha$ and $\delta\alpha'$ are both positive (negative, for odd N). Therefore the sequence of successive α_j's is monotonic (growing for even N, decreasing for odd N). Moreover the α_j's vary very slowly in the limit of large N [remember that $F_N\simeq(1+\sigma)^N$].

In the case $1/F_N\ll\varepsilon\ll 1$, $\mu\notin[\mu_1^0,\mu_2^0]$ but is chosen so that W still belongs to $[W_1,W_2]$. Again we define $\mu/(F_NF_{N+1})$ in the vicinity of Farey neighbors F_{N-2}/F_N and F_{N-1}/F_{N+1} by

$$\mu/(F_NF_{N+1})=F_{N-2}/F_N-\chi\varepsilon/F_N$$
$$=F_{N-1}/F_{N+1}-\chi\varepsilon/F_N+1/(F_NF_{N+1}) \ ,$$

where χ is a finite arbitrary real.

Relations (23) and (24) are then replaced by

$$\delta\alpha=2\pi[2/F_N-\chi\varepsilon(2/\rho-3)] \ , \qquad (25)$$

$$\delta\alpha'=2\pi[1/F_N+\chi\varepsilon(2-1/\rho)] \ , \qquad (26)$$

where mod(2π) has been dropped. For $\chi\varepsilon\gg F_N$ we see that $\delta\alpha$ and $\delta\alpha'$ now have opposite signs. Therefore $\alpha_j$mod(2π) is no longer a monotonic sequence. Now it may be shown that, in the limit of large N, intervals m_j and m_k are uniformly distributed over the two intervals appearing in inequalities (22), whose lengths are $2P-Q$ and $2Q-3P$. We are therefore led to assign to sequences

(1),(2) probability weights ω_1,ω_2 proportional to the measure of these intervals. We thus obtain $\omega_1=(2\rho-1)/(1-\rho)$ and $\omega_2=(2-3\rho)/(1-\rho)$. Averaging over a large number of sequences, we obtain

$$\langle \delta\alpha \rangle=\omega_1\,\delta\alpha+\omega_2\,\delta\alpha'=(-1)^N(2\pi/F_{N+1}) , \tag{27}$$

where the $(-1)^N$ factor has been added to make the formula valid when N is odd. Let N_1 and N_2 be the total number of sequences (1) and (2) over one period. We have, in the limit of large N, $N_1/\omega_1=N_2/\omega_2$. Moreover, since sequences (1) and (2) are respectively produced by five and three mapping iterations, we have:

$$5N_1+3N_2=M=F_N+F_{N+1}-1\approx F_N+F_{N+1} ,$$

from which $N_1=(2\rho-1)F_{N+1}$, $N_2=(2-3\rho)F_{N+1}$, and the total number of sequences is $N_t=N_1+N_2=(1-\rho)F_{N+1}$. Finally, we find for the total variation of the averaged α over one period:

$$\Delta(\langle\alpha\rangle)=N_t\langle\delta\alpha\rangle=(-1)^N(2\pi) . \tag{28}$$

We conclude that, for large N, small ε and $W\in[W_1,W_2]$, $\alpha_j \bmod(2\pi)$ is a very slowly varying angle, always close to its averaged value $\langle\alpha_j\rangle$, except for small fluctuations of the order of ε. Our idea is to replace the exact angular mapping by a "coarse-grained" approximation of it, in which will only enters $\langle\alpha_j\rangle$. This will be done in the following way.

Let us write down the five iterations of angular mapping (14) associated with a sequence (1). At first order in ε we obtain

$$\theta_1=\theta-2\pi\mu P-2\varepsilon(1+\sin\theta) ,$$

$$\theta_2=\theta_1-\alpha-2\varepsilon(1+\sin\theta_1) ,$$

$$\theta_3=\theta_2-(2\pi\mu P-\alpha)-2\varepsilon(1+\sin\theta_2) ,$$

$$\theta_4=\theta_3-(2\pi\mu(Q-P)+\alpha)-2\varepsilon(1+\sin\theta_3) ,$$

$$\theta'=\theta_4-(2\pi\mu(2P-Q)-\alpha)-2\varepsilon(1+\sin\theta_4) .$$

Adding up these relations gives

$$\theta'=f_1(\theta)=\theta-2\pi\mu(3P)-2\varepsilon(5+\sin\theta+\sin\theta_1+\sin\theta_2+\sin\theta_3+\sin\theta_4) .$$

Similarly the three iterations associated with a sequence (2) yield

$$\theta'=f_2(\theta)=\theta-2\pi\mu(2P)-2\varepsilon(3+\sin\theta+\sin\theta_1+\sin\theta_2) .$$

We have therefore to iterate a sequence of mappings $f_1(\theta)$ and $f_2(\theta)$, corresponding to the ordered set of subsequences (1) and (2). We shall now assume $1/F_N\ll\varepsilon\ll1$ (it is the case where strong localizations are expected) and evaluate $f_{1,2}(\theta)$ at first order in ε. We have the following approximations:

$$\mu P=-\chi\varepsilon+O(1/F_N)\ [\bmod(1)] ,$$

$$\theta_1=\theta_3=\theta+O(\varepsilon) ,$$

$$\theta_2=\theta_4=\theta-\alpha+O(\varepsilon) .$$

Therefore we obtain at this order

$$f_1(\theta)=\theta+2\pi(3\chi\varepsilon)-2\varepsilon[5+3\sin(\theta)+2\sin(\theta-\alpha)] ,$$

$$f_2(\theta)=\theta+2\pi(2\chi\varepsilon)-2\varepsilon[3+2\sin(\theta)+\sin(\theta-\alpha)] .$$

The coarse-graining procedure will consist of adding and averaging over p sequences (1) and δp sequences (2), δ being the probability ratio ω_2/ω_1 and p being chosen such that $1\ll p\ll1/\varepsilon$. We shall neglect the α_j fluctuations (being of the order of ε) around their average value $\langle\alpha_j\rangle$. Therefore, in the following, α_j will have the meaning $\langle\alpha_j\rangle$ in the expressions for $f_{1,2}(\theta_j)$. Moreover, the $\langle\alpha_j\rangle$'s and θ_j's varying very slowly in the course of the averaging process, we shall neglect their variation during the iteration over the above set of (1) and (2) sequences (which induces a relative error $\delta\theta/\theta$ of the order of ε). We obtain in this way the unique mapping

$$\theta_{j+1}=F(\theta_j)=\theta_j+2\pi(3+2\delta)p\chi\varepsilon-2p\varepsilon[5+3\delta+(3+2\delta)\sin\theta_j-(2+\delta)\sin(\alpha_j-\theta_j)] ,$$

or

$$\theta_{j+1}=\theta_j+\varepsilon'[\gamma+\sin(\alpha_j-\theta_j)-(1/\rho)\sin\theta_j] , \tag{29}$$

where

$$\delta=(2-3\rho)/(2\rho-1)\quad(\delta\to\sigma \text{ for } N\to\infty) ,$$

$$\gamma=[2\pi(3+2\delta)\chi-2(5+3\delta)]/[2(2+\delta)] ,$$

$$\alpha_j=(-1)^N(2\pi j/\tilde N) ,$$

$$\tilde N=(1-\rho)F_{N+1}/[p(1+\delta)]\quad(\tilde N\to F_{N+1}/p \text{ for } N\to\infty) ,$$

$$\varepsilon'=2\varepsilon F_{N+1}/\tilde N ,$$

$$\lim_{N\to\infty}(1/\rho)=1+\sigma .$$

The last step will be, in the limit of large N, to treat θ and α as continuous variables. Replacing $\{\alpha_j,\theta_j\}$ by $\{\alpha,\theta\}$ in Eq. (25), and multiplying this equation by $\tilde N/2\pi$ yields, for $N\to\infty$, the following differential equation:

$$d\theta/d\alpha=A[\gamma+\sin(\alpha-\theta)-(1+\sigma)\sin\theta]\quad(N \text{ even}) , \tag{30}$$

with

$$A=\tilde N\varepsilon'/(2\pi)=\varepsilon F_{N+1}/\pi . \tag{31}$$

We shall first consider systems containing only one spatial period of the refractive index field; that is, $\alpha\in[0,2\pi]$.

In the case of odd N, the differential equation takes the same form, provided $\{\alpha,\theta\}$ is replaced by $\{\alpha'=-\alpha,\theta'=-\theta\}$, and γ by $-\gamma$. As expected the coarse-graining parameter p no longer appears in Eq. (30).

We are now in a position to investigate localized solutions. Let us first come back to expression (17) giving the energy of a solution as a function of the number of itera-

tions. Using the coarse-graining approximation, this expression reads

$$I_n \simeq \prod_{j=1}^{n} (1+2\varepsilon\cos\theta_j)^{p(3+2\delta)}[1+2\varepsilon\cos(\theta_j-\alpha_j)]^{p(2+\delta)} . \tag{32}$$

Since α_j varies monotonically in $[0,2\pi]$, we see that a solution peaked around the center of the system will be obtained if there exists a solution $\{\theta_j\}$ of the angular mapping (29) which is monotonic in $[0,\pi]$.

Numerical iteration of original mapping (14) (which is free of the coarse-graining approximation) shows that such solutions do exist, and their shape, for rational ρ, is sketched in Fig. 6. This graph contains three branches, one of them very close to the first diagonal, the two others close to the second diagonal. The iterated points are found alternatively on the three branches: Those near the first diagonal correspond to angles θ_j in the coarse-grained mapping, while the other ones correspond to $\theta_j-\alpha_j$. Obviously such an angular graph yields a localized state peaked around the center of the system; we call it the "fundamental localization." Finally, numerical iteration of the mapping over several periods suggests that point $(\alpha=2\pi, \theta=\pi)$ is homoclinic.

At energy values where numerical integration of the angular mapping showed the fundamental localization, we have calculated the orbits of the eigenvectors of $\mathring{A}_M(E,\varepsilon)$ by matrix multiplications. We have actually obtained intensities I_n which are symmetrical and peaked around the period's center. The width of localized states decreases with N, while the energy band where those states are found becomes exceedingly small at large N (for $N=15$, $\Delta\chi\simeq 10^{-10}$). Some numerical results are sketched in Fig. 7. Finally let us mention that these results are in excellent agreement with those obtained with the help of the coarse-grained Eq. (29).

We shall now show how these various properties proceed from the study of the coarse-grained mapping (29) or of the differential equation (30). Let us first consider mapping (29). It may be considered as an autonomous mapping depending on the slowly varying parameter α. For given α, its fixed points are given by

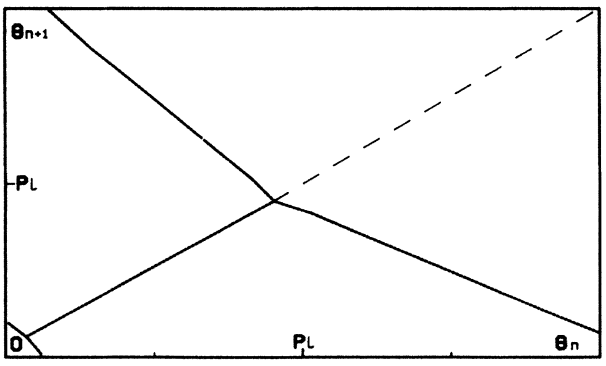

FIG. 6. Iteration of angular mapping (4) for a particular energy value giving the fundamental localization $N=12$, $\varepsilon=0.01$, and $\mu=33\,550.18$.

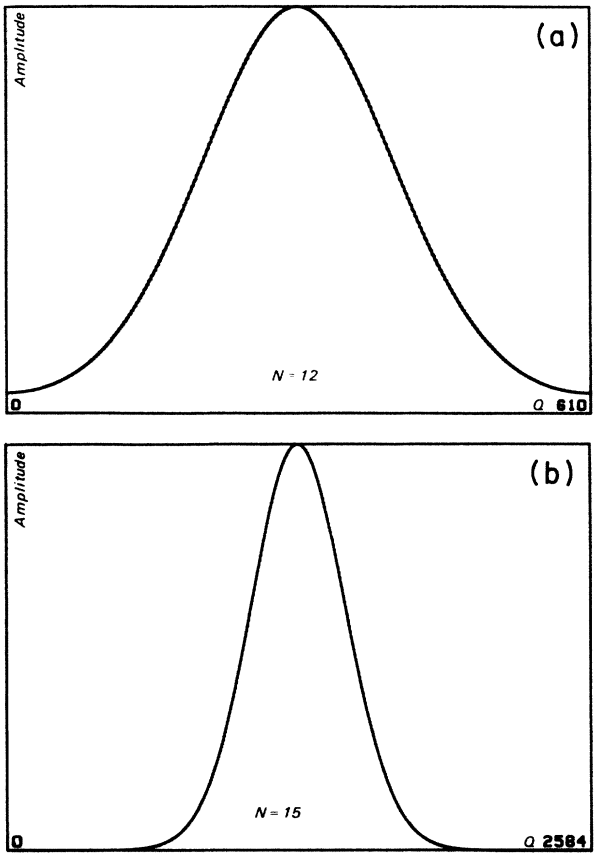

FIG. 7. The fundamental localization. Graphs of I_n as a function of n, obtained by numerical iteration of the matrix transformation. (a) $N=12$, $\varepsilon=0.01$, $\mu=33\,550.18$. (b) $N=15$, $\varepsilon=0.01$, $\mu=602\,063.155$.

$$H_\alpha(\theta)=\gamma+\sin(\alpha-\theta)-(1+\sigma)\sin\theta=0 .$$

(in the limit $1/\rho\to 1+\sigma$). There are in general two fixed points θ_1 and θ_2, one stable $(\partial H/\partial\theta_1<0)$, the other one unstable $(\partial H/\partial\theta_2>0)$. It is easily seen that, for $\alpha\in[0,2\pi]$, these fixed points do exist $\forall\alpha$ if $\gamma<\sigma$. For $\gamma>\sigma$ there exists an interval $[\alpha_1,\alpha_2]$ where they vanish; $\theta_1=\theta_2$ when α is equal to α_1 or α_2. For $\gamma=\sigma$, $\alpha_1=\alpha_2=\pi$ and $\theta_1=\theta_2=\pi/2$. Figure 8 shows the graph (A) of $H(\theta)$ for $\gamma=\sigma$ and a particular value of α $(\alpha=\pi/2)$ and the graph $B_\sigma(\alpha)$ of the minima of $H_\alpha(\theta)$ for $\gamma=\sigma$. $B_\gamma(\alpha)$ does not intersect the α axis for $\gamma<\sigma$, and there are two intersection points for $\gamma>\sigma$.

We see that, for $\alpha=\pi$, A touches the θ axis. When $\gamma<\sigma$, A always intersects the axis. For $\gamma<\sigma$, Γ stays above the axis when $\alpha\in[\alpha_1,\alpha_2]$. Let us first consider the case $\gamma<\sigma$. Starting with an arbitrary θ initial value at $\alpha=0$, the iteration of the mapping rapidly leads towards stable fixed point θ_1. Then we follow the fixed point as α is increased. This one attains a maximum value smaller than $\pi/2$, then goes back to zero. For $\gamma>\sigma$ we again follow θ_1 when α is increased up to α_1. Then the fixed points disappear, and iterating the mapping makes the point escape towards larger values so that it is found beyond the fixed points when they later reappear (for $\alpha=\alpha_2$).

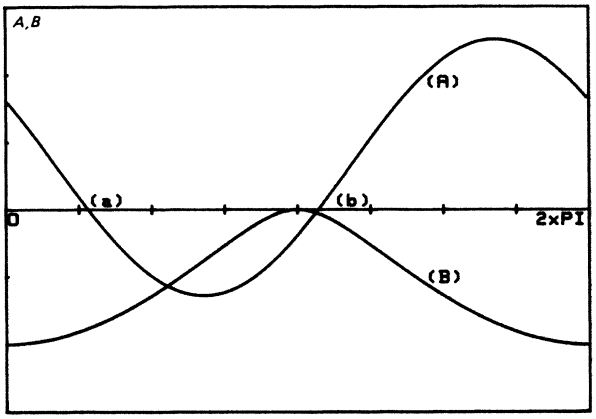

FIG. 8. Curve (A): graph of $H_{\pi/2}(\theta)$ for $\gamma=\sigma$. Curve (B): graph of $B_\sigma(\alpha)$ giving the minima of $H_\alpha(\theta,\gamma=\alpha)$. $B_\gamma(\alpha)$ is obtained from $B_\alpha(\alpha)$ by a translation parallel to the vertical axis.

In the two above cases the obtained solutions are not of the localized type. The only way of interpreting the numerical results above is that the orbit first follows stable fixed point θ_1 (up to $\alpha\approx\pi$) then sticks to the unstable point θ_2 (the explanation of this rather surprising situation will be found below). Such a "fixed point exchange" could *a priori* take place for $\gamma=\sigma$ (at $\alpha=\pi$, $\theta=\pi/2$), the choice between θ_1 and θ_2 being *a priori* undecided. However, we shall see below that for large but finite N, the "θ_2 solution" is chosen provided γ is taken to be slightly larger than σ. In this case we may understand that during the tiny interval $[\alpha_1,\alpha_2]$, a few iterations of the mapping makes the solution overtake the later-born unstable fixed point (see Fig. 9). Things will be made more precise by studying the differential equation. Let us first introduce the new variables $\xi=x-\pi$, $\varphi=\theta-\pi/2$, in terms of which Eq. (30) reads

$$d\varphi/d\xi=A[\gamma+\cos(\xi-\varphi)-(1+\sigma)\cos\varphi] \tag{33}$$

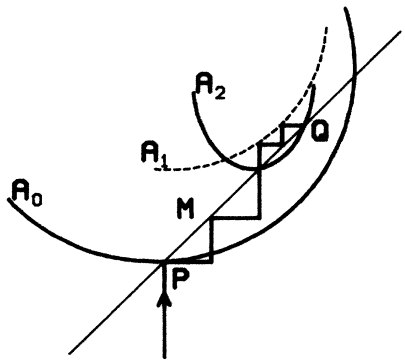

FIG. 9. Iteration of the angular mapping in the neighborhood of $\alpha=\pi$, and for γ slightly larger than σ. The three curves (A_0), (A_1), and (A_2) give the behavior of $\theta+H_\alpha(\theta)$ for $\alpha_0-\delta\alpha$, $\alpha_0+\delta\alpha_1$, and $\alpha_0+\delta\alpha_2$ (α_0 being the value where $\theta+H(\theta)$ touches the diagonal, and $\delta\alpha_2>\delta\alpha_1$). The solution point M moves right following stable fixed point $P(\alpha_0-\delta_\alpha)$, then the fixed points disappear ($\alpha_0+\delta\alpha_1$). When they reappear ($\alpha_0+\delta\alpha_2$), M has slightly overtaken unstable fixed point Q. Henceforth Q "pushes forward" point M as α increases.

with $\xi\in[-\pi,\pi]$.

A localized solution $\varphi(\xi)$ of the type obtained in numerical calculations would be such that (i) $\varphi(0)=0$ and (ii) φ variation is of the order of π when ξ goes from $-\pi$ to π. Condition (i) being satisfied, we remark that the graph of $\varphi(\xi)$ is symmetrical with respect to point (0,0), as it should be.

Satisfying condition (ii) in the limit of large N clearly implies that $\varphi(\xi)$ must be close to a solution $\psi(\xi)$ of the following equation:

$$\gamma+\cos(\xi-\psi)-(1+\sigma)\cos\psi=0\ . \tag{34}$$

Condition $\varphi(0)=0$ implying that $\psi(0)=0$, we must choose $\gamma=\sigma$ ($\gamma=-\sigma$ for odd N). There exist two solutions $\psi_{1,2}(\xi)$ of Eq. (34) for $\gamma=\sigma$, which are conveniently defined through their inverses. They read around the origin

$$\xi=\begin{cases}\psi+\beta(\psi) & (\xi>0)\ ,\\ \psi-\beta(\psi) & (\xi<0)\ ,\end{cases}$$

where

$$\beta(\psi)=\arccos[(1+\sigma)\cos\psi-\sigma]\ ,$$

$\psi_1(\xi)$ and $\psi_2(\xi)$ being defined by their derivative at $\xi=0$:

$$d\psi_1/d\xi\,|_{\xi=0}=(1+\sqrt{1+\sigma})^{-1}\ ,$$
$$d\psi_2/d\xi\,|_{\xi=0}=(1-\sqrt{1+\sigma})^{-1}\ .$$

As far as fundamental localization is concerned, we need only consider ψ_1 and ψ_2 for $\theta\in[-\pi,\pi]$. However, we shall later consider larger intervals. Then we must use the analytic continuation of the above function beyond the ξ values where $(1+\sigma)\cos\psi-\sigma=\pm1$. We thus obtain, on unbounded supports, that ψ_1 and ψ_2 are periodic functions of ξ with period 4π. The graphs C_1 and C_2 of $\psi_1(\xi)$ and $\psi_2(\xi)$ are sketched in Fig. 10.

We have the following properties: (i) $\psi_2(\xi)=\psi_1(\xi-2\pi)$; (ii) $\psi_{1,2}(\xi)=-\psi_{1,2}(-\xi)$; (iii) we observe that for $\xi\in[-\pi,\pi]$, ψ_1 varies almost linearly in ξ, and is approximately given by $\psi_1(\xi)\approx(\frac{1}{2}-\theta_0/\pi)\xi$, with $\theta_0=\arcsin(2\sigma-1)$. (iv) C_1 and C_2 are contained in the angular band $[-(\pi/2+\theta_0),(\pi/2+\theta_0)]$. (v) The set $\{\psi_i^k(\xi)\}$ ($i=1,2;k\in\mathbb{Z}$) of all the solutions of Eq. (34) is defined by $\psi_i^k(\xi)=\psi_i(\xi)+k(2\pi)$, their graphs C_i^k being obtained from C_i by $k(2\pi)$ translation along the θ axis.

We shall not give here the proof of the existence of solutions $\varphi_{1,2}(\xi)$ in the vicinity of $\psi_{1,2}(\xi)$. We shall instead show that one can construct without any contradiction a perturbative expansion of such solutions. We introduce a function $u(\xi)$ defined through its inverse according to

$$\xi+u=\varphi+\arccos[(1+\sigma)\cos\varphi-\sigma]=G(\varphi)$$
$$[G(\psi_i)=\xi;i=1,2]\ , \tag{35}$$

and the parameter $\nu=\gamma-\sigma$. We now expand φ,u,ν as

$$\varphi=\psi_i+\varphi_1+\varphi_2+\cdots ,$$

$$u=u_1+u_2+\cdots ,$$

$$\nu=\nu_1+\nu_2+\cdots ,$$

where the φ_j,u_j,ν_j are of the order of A^{-j}. Equation (32) can be rewritten as

$$\cos(\xi+u-\varphi)-\cos(\xi-\varphi)=\nu-(1/A)d\varphi/d\xi . \quad (36)$$

At first order in $1/A$, Eq. (36) gives $u_1(\xi)=[(1/A)d\varphi/d\xi-\nu_1]/\sin(\xi-\psi_i)$, and u_1 is made regular at the origin by choosing $\nu_1=(1/A)d\psi_i/d\xi$. Then Eq. (35) yields at first order $\varphi_1(\xi)=u_1(\xi)/G'(\psi_i)$, an expression which is regular in $[-\pi,\pi]$. The successive terms of the expansion are obtained in the same way from Eqs. (35) and (36), and they are not singular in $[-\pi,\pi]$. This has been made possible because $G(\psi)$ and all its derivatives are regular and do not vanish in this interval. Moreover, this perturbative expansion yields a unique solution of Eq. (33) in the vicinity of each ψ_i. Numerical integration of the differential equation confirms the existence of such solutions, even in the extended interval $[-2\pi,2\pi]$. Let us note that, in the frame of this expansion we obtain that $\gamma=\sigma+O(1/A)$, a value which is associated with $\chi=2/\pi+O(1/A)$; if N is odd the corresponding values are $\gamma=-\sigma$ and $\chi=2(3-4\sigma)/\pi+O(1/A)$ terms.

The localized solution corresponds to arc AB of Fig. 10. It extends over an interval $\Delta\theta=\pi-2\arcsin(2\sigma-1)$. Therefore the associated rotation number is irrational and the fundamental localization takes place, for a finite system, in a pass band. Let us determine the intensity profile of the localized solution. Taking the logarithm of relation (32), and going to the limit of continuous variables, we get

$$\ln[I(\xi)/I(0)] = -A\int_0^{\xi}\{\sin[\xi'-\varphi(\xi')]+(\sigma+1)\sin\varphi(\xi')\}d\xi' .$$

Choosing where the normalization constant I_0 has been chosen in such a way that $I(0)=1$ (maximum value). ξ and φ being related through relation (34) (with $\varphi\approx\psi_1$), the above formula yields the following expression of $\ln(I/I_0)$ in terms of φ:

$$\ln[I(\varphi)/I(0)]=(2A/\sigma)[F(\varphi)-F(-\varphi_m)] ,$$

where

$$F(u)=\cos u+2\cos(u/2)[\cos^2(u/2)-\sigma^2]^{1/2} ,$$

and

$$\varphi_m=\arccos(2\sigma-1) .$$

We obtain around $\varphi=\xi=0$

$$I(\xi)\approx\exp[-A\xi^2/(2\sqrt{\sigma})] .$$

Moreover we have, in the limit of large N:

$$\int_{-\varphi_m}^{\varphi_m} I(\varphi)d\varphi\simeq\int_{-\pi}^{\pi} I(\xi)d\xi\simeq A^{-1/2} ,$$

and, therefore, these integrals go to zero as $L^{-1/4}$ (remember that $A\simeq F_N\varepsilon$, and $L=lF_NF_{N+1}$). Now ξ is related to spatial variable x through $\xi/(2\pi)=x/L$. Therefore

$$\int_0^L I(x)dx=[L/(2\pi)]\int_{-\pi}^{\pi} I(\xi)d\xi\simeq L^{3/4}$$

for large N. Then $\int_0^L I(x)dx\to\infty$ as $L\to\infty$, and we cannot qualify $\varphi(\xi)$ as a localized solution (according to the usual definition). Defining the "sojourn time" T_Λ in a box Λ as being proportional to the ratio (energy stored in Λ)/(energy flux), one easily finds that $T_\Lambda\to\infty$ when $L\to\infty$. Since a Floquet solution can be constructed by adding up two independent class-W solutions enjoying the above properties, we conclude that the energy of such a solution belongs to the singular continuous part of the energy spectrum. We also remark that the average stored energy $(1/L)\int_0^L I(x)dx$, or the relative width $\Delta x/L$ of the solution support, goes to zero like $L^{-1/4}$ for large L. In this limit, $\varphi(\xi)$ looks strongly peaked around $\xi=0$ [see Fig. 6(b)], that this is localized is common sense for the physicist. For this reason, we shall call $\varphi(\xi)$ a "quasilocalized" solution. We also observe that this solution exhibits no recurrent behavior. This is in contradistinction with the solutions of a class of Schrödinger equations whose potential is the sum of equidistant peaks with quasiperiodic amplitude (cf. the Delyon and Petritis theorems).[6]

The above arguments justify the existence of solutions $\varphi_{1,2}(\xi)$ of the differential equation in the neighborhood of $\psi_{1,2}(\xi)$. Now it is important to study the stability of these solutions with respect to a variation of the initial condition and of γ. We shall show that the $\xi>0$ ($\xi<0$) branch of ψ_1 (ψ_2) is stable, while the symmetric branch is unstable.

Linearizing Eq. (32) around $\varphi_i(\xi)$ ($i=1,2$), we obtain

$$\{d/d\xi-A[\sin(\xi-\varphi_i)+(1+\sigma)\sin\varphi_i]\}y_i=A\delta\gamma , \quad (37)$$

where $\delta\gamma$ is the deviation of γ from the above exact value $(\sigma+\nu)$. At lowest order with respect to $1/A,\varphi_i(\xi)$ will be replaced by $\psi_i(\xi)$ and this equation reduces to

$$\{d/d\xi-A\sin(\xi-\psi_i)/(d\psi_i/d\xi)\}y_i=A\delta\gamma . \quad (38)$$

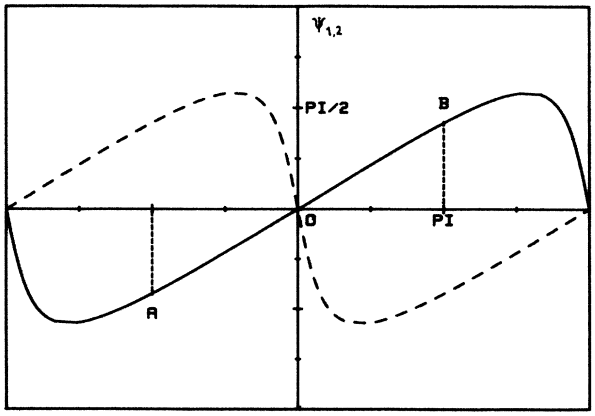

FIG. 10. Graphs of C_1 and C_2 of $\psi_1(\theta)$ and $\psi_2(\theta)$.

We first ignore the deviation $\delta\gamma$ (i.e., we take $\delta\gamma=0$ in the equation), and only consider the effect of a deviation y_i^0 from initial value $\varphi_i(-\pi)$. Then the solution of Eq. (37) reads

$$y_i(\xi)=y_i^0\exp\left\{\int_{-\pi}^{\xi}\sin[\xi'-\psi_i(\xi')]/(d\psi_i/d\xi')d\xi'\right\}.$$

We see that, for $i=1$, the integrand is negative (positive) for $\xi<0$ ($\xi>0$). This shows that the negative branch of $\varphi_1(\xi)$ is stable with respect to initial conditions (attractive branch), while the positive branch is unstable. Opposite conclusions are valid for $i=2$.

As a consequence, the orbit of any initial state is localized. The fundamental localized solution, in terms of angular variable, is the orbit of initial value $\varphi(-\pi)=\pi/2-\theta_0$ (point A of Fig. 8); it corresponds to arc AB of curve C_1. Now any initial point in the $\{\theta_n\to\theta_{n+1}\}$ coarse-grained graph will be rapidly attracted towards the C_1 curve, then will stick to it up to the end of the period. Therefore any state Y belonging to class W has a localized orbit. In the general case of a state not belonging to W, it can be projected over two independent class-W states and its orbit is therefore localized.

Solving Eq. (38) yields more detailed and important information. Since $\psi_i(\xi)$ is symmetrical with respect to the origin, y_i is an even function of ξ. Using the approximate linear expression for $\psi_1(\xi)$, y_1 is given by

$$y_1(\xi)=y_1^0\exp(-\tilde{A}\{\cos[(1+2\theta_0/\pi)\xi/2]+\sin\theta_0\}) \quad (39)$$

with

$$\tilde{A}=4A/[1-(2\theta_0/\pi)^2].$$

The orbit of any initial point $(-\varphi_0,-\xi_0)$ stays in the neighborhood of (C_1) up to $\xi=\xi_0$. Therefore, for $\xi\in[0,\xi_0]$, the orbit point "follows" the unstable fixed point.

Let us now investigate the sensitivity of the localized solution versus an energy shift $\delta\gamma$. Integrating Eq. (38) with $y_1^0=0$ as the initial value and using again the linear approximation for $\psi_1(\xi)$, we obtain the following deviation:

$$y_1(\xi)=A\delta\gamma\int_{-\pi}^{\xi}\exp(\tilde{A}\{-\cos[(1+2\theta_0/\pi)\xi/2]+\cos[(1+2\theta_0/\pi)\xi'/2]\})d\xi'.$$

This reduces in the limit of large A and for $\xi>0$, to

$$y_1\simeq\delta\gamma\,\tilde{A}^{1/2}e^{\tilde{A}\{1-\cos[(1+2\theta_0/\pi)\xi/2]\}}. \quad (40)$$

We see that $y_1(\xi)$ grows very rapidly for $\xi>0$. A necessary condition for preserving the localized solution is obviously that $|y_1|$ stays smaller than or of the order of unity in $[-\pi,\pi]$. Imposing that the variation of $|\theta_{n+M}-\theta_n|$ be smaller than 2π would give approximately the same condition, and this condition fixes the width $\Delta\mu$ of the fundamental pass band. This condition reads

$$\delta\gamma<\delta\gamma_{\max}\simeq\tilde{A}^{-1/2}e^{-\tilde{A}}. \quad (41)$$

One may consider a finite propagative system (associated with a given value of N) as a resonator, whose resonant frequency belongs to the fundamental pass band. One can assign to this resonator the quality factor $Q=\delta\gamma_{\max}^{-1}$. Remembering that $\tilde{A}$ is proportional to $\varepsilon F_{N+1}\simeq\varepsilon\sqrt{L}$ (L denotes the spatial extension of system's period), we see that $Q\simeq\varepsilon^{1/2}L^{1/4}e^{a\varepsilon\sqrt{L}}$, a being a numerical coefficient. This suggests that propagative mediums with modulated refractive index of model A type could be interesting candidates for realizing high-resolution frequency filters.

A last consequence of the above results is the following. Remember that for large but finite N, the graph $\theta_n\to\theta_{n+1}$ is aperiodic, since the energy has been chosen inside a pass band. Iterating over several periods of the system (that is, considering $\xi>\pi$ in the differential equation), we see that the instability of $\varphi_1(\xi)$ for $\xi>\pi$ explains the homoclinic behavior of point (π,π) in the above mapping. Concerning the solution of Eq. (33) for $\xi>\pi$, two possible behaviors are expected when energy is slightly varied: (i) The orbit leaves C_1 at point B (see Fig. 11), and falls on C_2 in A_1, or (ii) the orbit runs along BA_1', passing from C_1 to C_2^1: such a trajectory goes through the "forbidden angular gap" $[\pi/2+\theta_0,3\pi/2-\theta_0]$ between C_i and C_i^1.

The further trajectory will be either arc A_1B_1 on C_2 [case (i)], or arc $A_1'B_1'$ on C_2^1 [case (ii)]. The parameters controlling the choice between the two solutions are obviously the energy and the initial phase. Around $\xi=\pi$, deviation $y(\xi)$ from $\psi_1(\xi)$ becomes quite large and is the sum of the two contributions, (39) and (40), representing, respectively, the effect of the initial condition and of the energy shift. We see that the sign of y is determined by those of y_1^0 and $\delta\gamma$, and also, if $y_1^0\delta\gamma>0$, by the relative weight of y_1^0 and $|\delta\gamma|\sqrt{A}$.

Considering now a system containing an arbitrary number of periods, say m, we see that the orbit of a given initial state will be the union of m successive arcs A_kB_k belonging to C_i^k curves. How are these arcs distributed over the set of C_i^k's? Answering this question amounts to finding the set $\{k\}$ of corresponding integers. Determining the dependence of $\{k\}$ on parameters y_0 and $\delta\gamma$ could seem *a priori* a difficult problem. Indeed the successive finite jumps from a C_i^k curve to the next one can-

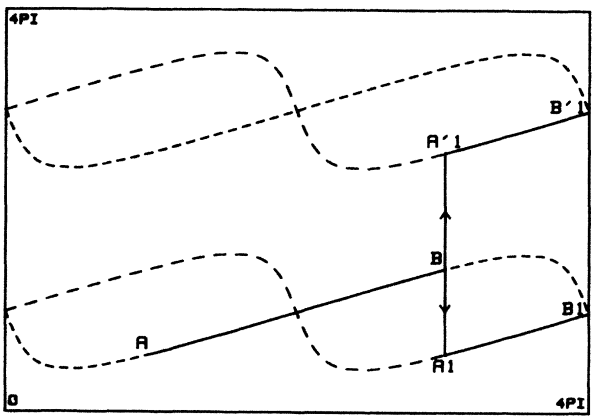

FIG. 11. Bifurcation from curve C_1 to either C_2 or C_1^2.

not be derived from linearized Eq. (37). However, one can show that, at given energy, any set $\{k\}$ may be deduced from two particular sets $\{k\}_1$ and $\{k\}_2$. Indeed, let us consider eigenstates $\mathbf{u}_1$ and $\mathbf{u}_2$ of $\mathring{A}_M(E,\varepsilon)$ with Λ_1 and Λ_2 orbits (they are the fundamental Floquet solutions). It is easily seen that angular variable φ associated with Λ_1 and Λ_2 orbits is periodic with period M, and the corresponding sets $\{k\}_1$ and $\{k\}_2$ are also periodic. Now any given initial state $\mathbf{Y}$ can be projected over $\mathbf{u}_1$ and $\mathbf{u}_2$ and it's orbit Λ is a linear combination of Λ_1 and Λ_2. Generically Λ is aperiodic and so is the associated set $\{k\}$ which is obtained from $\{k\}_1$ and $\{k\}_2$. A typical angular graph is sketched on Fig. 12.

Secondary localizations

The fundamental localization has been found between the dominant stop bands which are closest neighbors. Now the μ-energy spectrum of dominant SB's contains, in the limit $\varepsilon\to 0$, all the discrete x_j's (frontier abcissas). These values delimitate energy bands with widths $1,2,\ldots,P-1$; two for each band m, except for band $m=P$ (as was said before). The energy distribution of these bands is nothing but that of interpeak distances of the refractive-index field. An analytic expression for the energy intervals of the two mth bands is given, in the limit $\varepsilon\to 0$, in Appendix B. They are $E_m^{(i)}\pm 2\pi m/F_{N+1}$ $(i=1,2)$, with

$$E_m^{(1)}/2\pi = W_m^{(1)} = mF_N/F_{N+1} - \mathrm{Int}(mF_N/F_{N+1}) , \qquad (42)$$

and

$$E_m^{(2)}/2\pi = W_m^{(2)} = 1 + \mathrm{Int}(mF_N/F_{N+1}) - mF_N/F_{N+1} , \qquad (43)$$

where W_m is the rotation number associated with E_m.

For $m\in[1,P]$, we have a set of pairs of dominant stop bands whose rotation numbers $W_m^{(i)}$ respectively differ, in each pair, by $1/M, 2/M, \ldots, P/M$. Note that this band contains m secondary stop bands and therefore m adjacent pass bands. It must also be clear that any low-order band ($m \ll F_N$) is characterized by its averaged energy or rotation number, which is given by formula (42) or (43), *but its energy width is not m* (in unit μ), even for small ε. We shall come back to this point later.

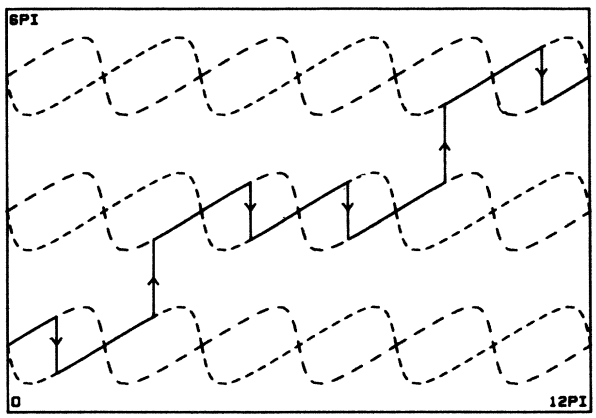

FIG. 12. A typical solution in a multiperiodic system (fundamental localization) or , equivalently, secondary localization in one period.

Choosing μ in one of these P energy bands, we observe exactly the same type of properties as in the fundamental band (quasimonotonic and slow variation of the α_j's, etc.). The only difference is that the drift speed of the $\langle\alpha_j\rangle$'s is modified. For instance the $\langle\alpha_j\rangle$ variation over a period, in the mth energy band, is $2m\pi$ instead of 2π. The coarse-graining procedure is still applicable, although its accuracy decreases when m is increased: Indeed, α_j varies more and more rapidly which makes the neglect of α_j's fluctuations in the averaging process less and less justified. The approximation remains good as long as m is sufficiently smaller than P.

Concerning the differential equation obeyed by the mth localization, it is the same as Eq. (33), provided that we make the scale transformations $\xi\to m\xi$ and $A\to A/m$, and remember that ξ varies in an interval of extension $2m\pi$. Therefore, all that was said in the preceding section on the localized solutions in a system containing m periods of $\nu(x)$ remains valid here. In other words there is a one-to-one correspondence between the solutions of a one-period system with an energy chosen in the mth energy band and those of an m-period system with corresponding appropriate energy lying in the fundamental pass band. Numerical two-peak and three-peak solutions, obtained by iterating matrix transformation (1) for energy values, respectively, taken in the second and third energy bands are shown in Fig. 13.

Finally we remark that formula (41), which was said to give the order of magnitude of the fundamental pass band width, can be applied in the case of an mth-order energy band, provided $\tilde{A}$ is replaced by $\tilde{A}/m$. This shows that the bandwidths grow rapidly with m and that finite pass bands ΔE are expected for $m > \varepsilon F_N$ ("finite" meaning that ΔE is not very small compared to unity: Remember that $E/(2\pi)\in[0,1]$). As a consequence we see that model-A finite systems are easily transparent. In particular, the nearest pass bands encountered around the fundamental ones are the largest.

MODEL *B*

Slowly varying phase shifts and intermittency

This model does not possess the symmetry of model A, but it keeps the fundamental property that ϕ_n [mod(2π)] is still a slowly varying variable for appropriate energy values.

Let us put $\rho n = r_n + c_n$, where $r_n = \mathrm{Int}(\rho n)$. According to relation (8) we have $\zeta_n = c_n \mathrm{mod}(1)$. Evaluating now the phase shift $\phi_n \mathrm{mod}(2\pi)$, we write in terms of energy E defined by Eq. (5)

$$2\phi_n/2\pi = E\zeta_n = Ec_n \ [\mathrm{mod}(1)] .$$

If $E/2$ is an integer, we also have

$$2\phi_n/2\pi = E(r_n + c_n) = E\rho n \ [\mathrm{mod}(1)] . \qquad (44)$$

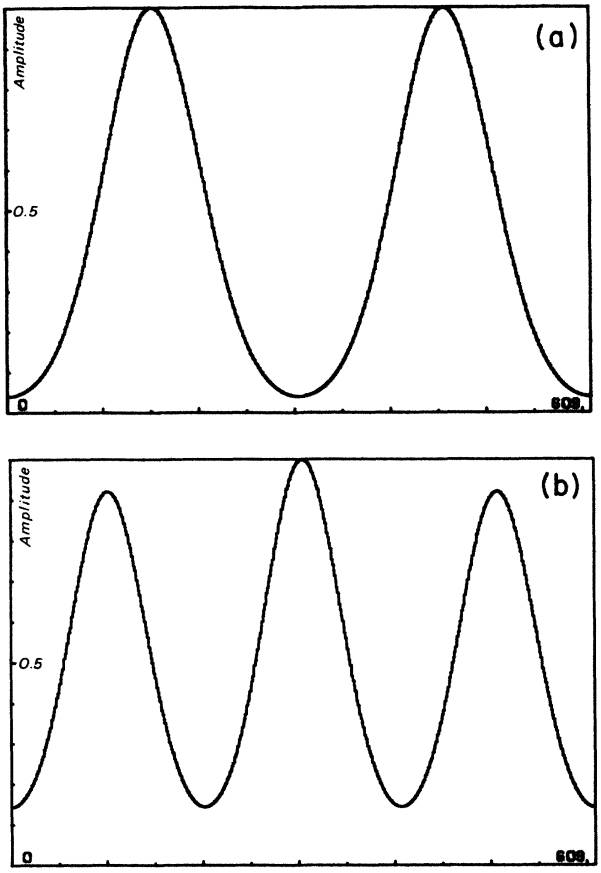

FIG. 13. Secondary localizations obtained by numerical iteration of the matrix transformation. (a) Second-order localization: $N=12$, $\varepsilon=0.01$, $\mu=20\,732.94$. (b) Third-order localization: $N=12$, $\varepsilon=0.01$, $\mu=12\,811.8$.

We shall now show that $\phi_n[\mathrm{mod}(2\pi)]$ is made a slowly varying function of n if $E=F_N$ (a Fibonacci number). Taking indeed $\rho=\sigma$ (we shall only consider this case in the following) and using formula

$$F_N=[\sigma^{-(N+1)}+(-1)^N\sigma^{(N+1)}]/\sqrt{5}\ ,$$

we obtain $\sigma F_N=F_{N-1}+(-1)^N\sigma^N$, from which

$$[2\phi_n \bmod(2\pi)=\{2\pi[(-1)^N\sigma^N n]\bmod(1)\}\ .$$

In the limit of large N the graph $\phi_n\rightarrow\phi_{n+1}$ $[\mathrm{mod}(2\pi)]$ is stuck to the first diagonal. $2\phi_n$ $[\mathrm{mod}(2\pi)]$ varies very slowly and monotonically, growing or decreasing according to the parity of N. For $\rho=\sigma$ ϕn is aperiodic and the number of iterations needed for running through $[0,2\pi]$ is very close to $\tilde{N}=\sigma^{-N}$.

For such an energy value angular mapping (14) may be looked at as an autonomous one depending on the slowly varying parameter ϕ. This situation is analogous to those found in model A, and even simpler since the variable parameter is simply associated with a translation (or a rotation on the circle). As a consequence we shall not need to assume ε small.

Let us consider the fixed points of this mapping for given ϕ. They satisfy to $\phi=-\beta(\theta)$. The graph (B) of $-\beta(\theta)$ is sketched on Fig. 14. B is tangent to the θ axis

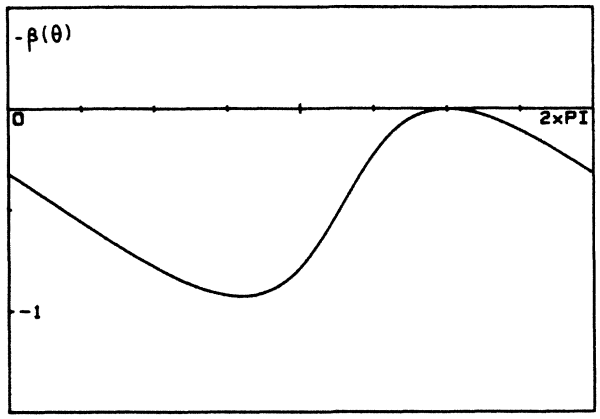

FIG. 14. Graph (B) of $-\beta(\theta)$.

at $\theta=3\pi/2$ and has a minimum at

$$\theta_c=\pi/2+2\lambda\ \ [\lambda=\arctan(\varepsilon)]\ , \tag{45}$$

with

$$\beta(\theta_c)=-2\lambda\ . \tag{46}$$

Therefore there exist two fixed points θ_1 and θ_2 as long as ϕ belongs to angular band $[-2\lambda,0]$. $\theta_1\in[\theta_c,3\pi/2]$ corresponds to the unstable fixed point, and $\theta_2\in[3\pi/2,2\pi]\cup[0,\theta_c]$ corresponds to the stable fixed point. Considering the local growth rate of intensity I_n defined by

$$\gamma_n=I_n/I_{n-1}\ ,$$

we have from formula (17), $\gamma_n=1+2\varepsilon\cos\theta_n+2\varepsilon^2(1+\sin\theta_n)$. It easily seen that $\gamma_n<1$ ($\gamma_n>1$) in the θ_1 (θ_2) domain.

We may now easily give a qualitative description of the solutions. They will be found by following "adiabatically" the local solutions obtained at constant ϕ. Let us assume $\phi_0=0$ and that ϕ is decreasing (odd N). Starting from an arbitrary initial value θ_0 for θ, we rapidly reach fixed point θ_1 and follow it up to θ_c. In this "fixed-point domain" (FPD) where $\phi\in[0,-2\lambda]$, intensity I_n grows monotonically. When $\phi<-2\lambda$, fixed points disappear; then we enter an "oscillatory domain" (OD) in which, as we shall later see, the orbit runs along a set of successive periodic cycles. For $\rho=\sigma$ the orbit is aperiodic and, when ϕ goes again beyond zero, θ reenters the fixed point regime with an "initial value" different from θ_0. In this way we get an intermittent solution in which oscillatory and monotonic paths alternate, the quasiperiod of the intermittency being $\tilde{N}$. As in model A exceptional orbits exist such that the chosen fixed point at the beginning of a FPD is the unstable one, making I_n decrease. In Fig. 15 numerical iteration of the mapping shows typical intermittency.

Pseudocycles and "noise localization"

When ϕ_n belongs to the OD, the eigenvalues of the nth transfer matrix A_n are complex and of the form $e^{\pm if_n}$, where $f_n=\arccos(\mathrm{Re}\alpha_n)$ (see preceding section). In

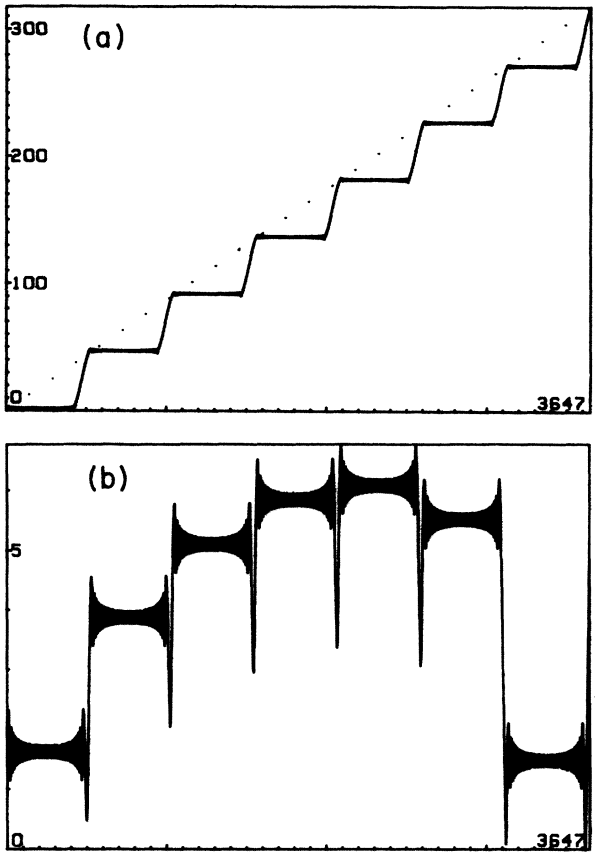

FIG. 15. (a) Typical intermittent solution. Graph of $\ln(I_n)$ as a function of n. One observes the regular staircase with wavy steps. (b) Graph of I_n for small ε. When an appropriate phase value is encountered at the end of an oscillatory domain, the solution escapes from the stable fixed point.

terms of parameter λ, f_n reads

$$f_n = \arccos[\cos(\phi_n + \lambda)/\cos\lambda] \ .$$

Let us now consider the wave propagation for $n \in [n, n+p]$, p being such that

$$1 \ll p \ll 1/a \quad \text{with } a = 2\pi\sigma^N \ . \tag{47}$$

It can be shown that, in the limit of large N, the transfer matrix

$$\mathring{A}_n^{n+p} = \prod_{j=n}^{j=n+p} A_j \approx (A_n)^p$$

at first order with respect to parameter ap. Performing the matrix multiplication in the above relation gives

$$\mathring{A}_n^{n+p} \approx \begin{bmatrix} \alpha_{np} & \beta_{np} \\ \beta_{np}^* & \alpha_{np}^* \end{bmatrix}$$

with

$$\alpha_{np} = e^{ipf_n} + [\sin(\phi_n + \lambda)/\cos\lambda - \sin f_n] \times [i \sin(pf_n)/\sin f_n] \ , \tag{48}$$

$$\beta_{np} = [i\varepsilon/(1+i\varepsilon)] \sin(pf_n)/\sin f_n \ . \tag{49}$$

We see that $\mathring{A}_n^{n+p} = 1$ whenever $f_n/2\pi = s/p$ (s arbitrary integer), and this situation corresponds to the existence of a period-p cycle for the mapping. Since $\phi_n \in [-2\lambda, -\pi]$ in the OD, $0 < f_n/2\pi < \frac{1}{2}$ and therefore $p/s \geq 2$. This means that p can take any integer value larger than or equal to 2.

At the center of the OD ($n = n_0$), $\phi_{n_0} = -(\pi/2 + \lambda)$, $f_{n_0}/2\pi - \frac{1}{4}$ (corresponding to a period-4 cycle), and we have $f_{n_0+n'} = f_{n_0-n'}$. Therefore the cycle set obtained by making $f_n/2\pi$ take all possible rational values in the OD is symmetrical with respect n_0. We also observe that a period-p cycle is obtained by only fixing ϕ; that is, independently of the chosen initial θ value. This means that, if $f_n/2\pi = s/p$ (fixing ϕ at the corresponding value), all the orbits of the mapping are periodic with the same period p, and therefore are not attracting: a property which is reminiscent of the linear character of the original matrix transformation. Clearly these results could be obtained from the study of the angular mapping, but in a much more intricate way.

Actually, since ϕ_n vary at each iteration, any orbit would "see" an infinite set of cycles corresponding to successive rational values taken by $f_n/2\pi$. As a result, at large but finite N, only the short-period cycles are actually observable. Indeed let n_p be the n value corresponding to a large period-p cycle, after a few iterations of the mapping, ϕ_n has already shifted from ϕ_{n_p}, making this cycle unobservable. On the contrary ϕ_n is nearly constant along several periods of a short cycle. We therefore expect a complicated or "noisy" behavior of any orbit in the OD, unless $f_n/2\pi$ is close to simple rational values. This idea will be made more precise by studying the solutions around $n = n_0$, at the center of the OD.

Let us make the change $n \to n_0 + n$; with

$$an \ll 1 \ ,$$

we have (50)

$$f_n \approx \pi/2 + an/\cos\lambda \ .$$

Now we shall extend the preceding calculation to the case where

$$\psi_n = f_1 + f_2 + \cdots + f_n = n(n-1)a/(2\cos\lambda) + n\pi/2$$

is such that $\psi_n - n\pi/2$ is finite. This is not contradictory with condition (50) provided that $a\cos\lambda \ll 1$. Then we get the following expression for the coefficients of transfer matrix $\mathring{A}_0^n$:

$$\alpha_{0n} = e^{i\psi_n} + i[\sin(\phi_0 + \lambda)/(\cos\lambda \sin f_0) - 1] \sin\psi_n \ , \tag{51}$$

$$\beta_{0n} = [i\varepsilon/(1+i\varepsilon)] \sin\psi_n / \sin f_0 = i \sin\lambda e^{-i\lambda}/\sin f_0 \tag{52}$$

with, here, $f_0 = \pi/2$ and $\phi_0 + \lambda = -\pi/2$. Let us now consider the propagation of initial state

$$\mathbf{u} = (e^{i\alpha/2}, e^{-i\alpha/2})/\sqrt{2} \ .$$

I_n, the intensity of $\mathbf{u}$'s orbit at nth iteration, exhibits a period-2 cycle (while the period of the θ cycle is 4). A straightforward calculation shows that I_n takes different

values according to the parity of n. We obtain

$$I_n = 1 + \nu \sin^2[n(n-1)a/(2\cos\lambda)] \quad (n \text{ even}),$$

$$I'_n = 1 + 2\varepsilon \sin\alpha + 2\varepsilon^2(1+\cos\alpha) - \nu \sin^2[n(n-1)a/(2\cos\lambda)] \quad (n \text{ odd}),$$

with

$$\nu = \sin^2\lambda + (1 - 1/\cos\lambda)^2 .$$

The graphs of I_n and I'_n are sketched on Fig. 16. I_n and I'_n exhibit, respectively, a minimum and a maximum for $n = n_0$. One observes that if α verifies the relation $\sin\alpha + \varepsilon(1+\cos\alpha) = 0$, or $\alpha = \lambda/2 + 3\pi/4$, the extrema of I_n and I'_n coincide. When this condition is realized, the intensity near $n = n_0$ is nearly constant; that is, nonfluctuating. Aside from an interval Δn of the order $a^{-1/2}$ around n_0, I_n is rapidly fluctuating, until another value of n is found where $f_n/2\pi$ is again a simple rational. We call this effect "noise localization." Note that its width Δn is small compared with intermittency length (which is of the order of a^{-1}). Noise localization is best shown on the graph of $\Theta_n = (\langle I_n^2\rangle - \langle I_n\rangle^2)/\langle I_n\rangle^2$, i.e., I_n's variance, $\langle\ \rangle$ meaning an average taken on δn such that $1 \ll \delta n \ll \Delta n$. Figure 17 shows a graph of Θ_n^{-1}.

More about intermittency

We have seen that the graph of θ_n solutions consists of an aperiodic sequence of "oscillating plateaus" (OD) connected by monotonic arcs (FPD). The ratio between FPD and OD widths is nearly $2\lambda/(\pi - 2\lambda)$. In general one follows the stable fixed point in the FPD and increasing I_n are observed yielding a solution whose shape is a regular staircase with wavy steps (see Fig. 15). However decreasing branches for I_n can be obtained also for convenient θ initial values: Then the unstable fixed point is chosen. Now one must also remember that the most general solution is obtained as an arbitrary sum of the orbits

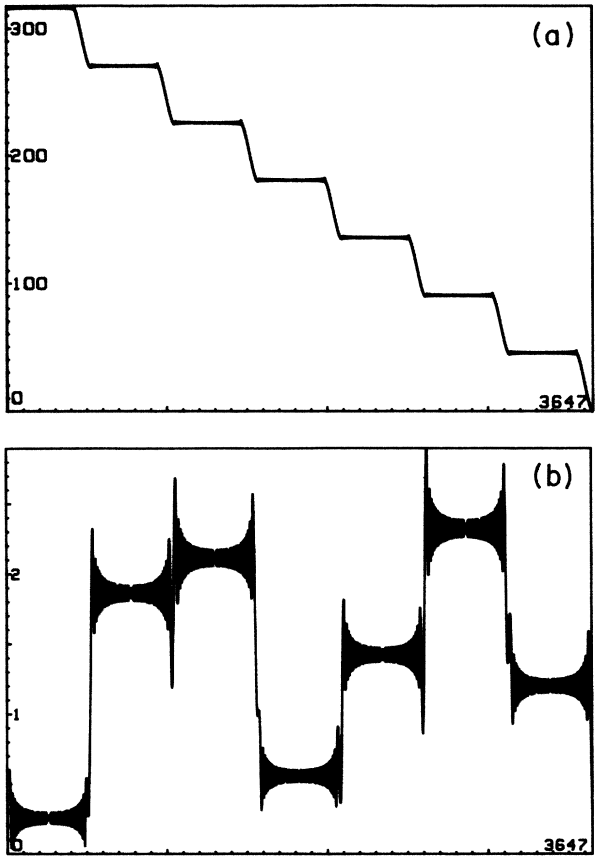

FIG. 17. Graph of I_n in a finite system illuminated from left side: (a) in a stop band ($E = 233$, $\varepsilon = 0.3$); (b) in a pass band ($E = 233$, $\varepsilon = 0.02$).

of two independent class-W states, and its shape strongly depends on boundary conditions. Consider for instance a large but finite system illuminated from the left side. Then energy conservation implies that $I_t = I_0(1-R)$, I_t being the transmitted wave intensity and R the reflexion coefficient: This prevents the solution to be of the ever-increasing type above. In particular I_t is finite and not

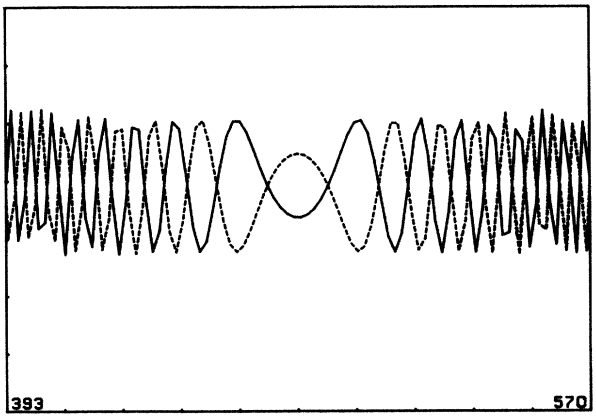

FIG. 16. Period-4 cycle (middle of an OD). Graph of the intensities I_n and I'_n obtained, respectively, for even and odd values of n. If the initial phase is conveniently chosen, the maximum of I_n and the minimum of I'_n coincide.

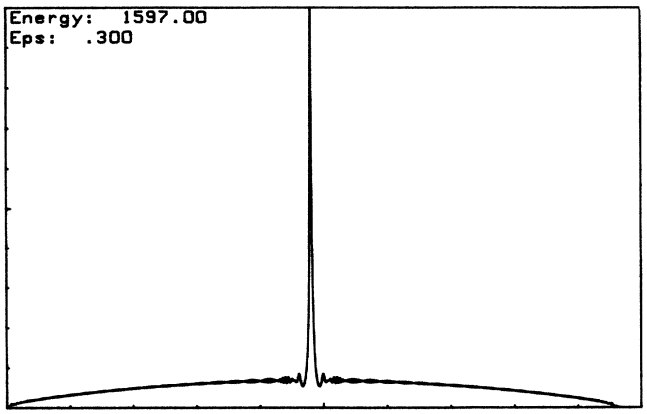

FIG. 18. Noise localization. Graph Θ_n^{-1} of the inverse variance of the "orbit noise" in the period-4 cycle domain (logarithmic scale).

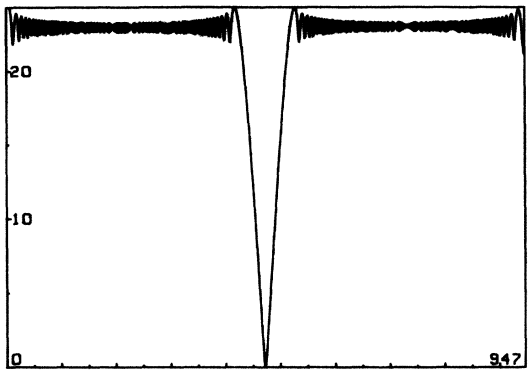

FIG. 19. Antilocalization. Graph of $\ln(I_n)$ in the oscillatory domain, with appropriate initial phase ($E=233$, $\varepsilon=0.3$).

vanishing when the energy belongs to a pass band (see Fig. 18).

Whatever be the particular solution considered, it is interesting to determine the total growth (or decrease) Γ of the intensity in a FPD. From relation (17) we have:

$$\Gamma=\sum_n \ln[\gamma(\theta_n)] ,$$

where the sum is extended over the FDP width. Going to the limit of continuous variables, we get, in a growing FPD

$$\Gamma=a^{-1}\varepsilon\int_{3\pi/2}^{5\pi/2+\lambda} H(\theta)/[1+2\varepsilon H(\theta)]d\theta ,$$

with

$$H(\theta)=\cos\theta+\varepsilon(1+\sin\theta) .$$

Γ is of the order of a^{-1} for finite ε, while, in the limit $\varepsilon\to 0$, $\Gamma\approx\pi\varepsilon^2 a^{-1}$. A last type of solution may be called "antilocalization", and is associated with a θ graph of the type shown on Fig. 19: One successively follows, in the FPD, the unstable fixed point, then the stable one. The parameter to be matched is obviously the initial phase.

Antilocalization and noise localization have been obtained by choosing precise values of the initial phase θ_0 and of the energy ($E=F_N$). It can be shown that θ_0 is extremely critical (much more than E), a situation opposite to that of model A. This suggests the use of model B propagative systems to detect ultrasmall phase shifts.

All the above results have been obtained by studying the discrete angular mapping. As could be expected, the slow variation of ϕ makes it possible, as in model A, to derive a differential equation obeyed by $\theta(x)$ in the limit of continuous variables. This is done in Appendix C. Making the variable change $\theta\to\theta+\lambda$, $\phi\to\phi+\lambda$, this equation reads

$$(a\sin f/2f)d\theta/d\phi-\sin\lambda\cos\theta=\sin\phi/\cos\lambda , \quad (53)$$

where

$$f=\arccos(\cos\phi/\cos\lambda) . \quad (54)$$

This is a nonautonomous differential equation, which can be formally integrated. Further detailed features of the solutions could of course be available from the integrated solution, but the main ones have already been obtained.

COMPARING THE MODELS AND CONCLUDING

The basic property, common to models A and B and explaining the phenomena described in this paper, is the slow variation of the phase shifts [mod(2π)] for convenient energy values. This property endows the quasiperiodic medium with strong regularity and makes the wave propagation highly organized. However, the two models are substantially different as regards the localization process.

Only model A is able to yield pseudolocalization of the wave energy. Indeed, some solutions in model B could seem to exhibit a "localized behavior." This happens when an OD is surrounded by two different FPD's (I_n growing into the left one and decreasing into the right one). However the ratio of OD width to intermittency quasiperiod is finite (of the order of ε for small ε). Therefore such solutions are not pseudolocalized [$\int I(x)dx$ is proportional to the system length]. In model B, fixed point domains necessarily alternate with finite oscillatory domains while, in model A, the averaged angular variable exhibits a monotonic evolution all along each half-period. Therefore, in model A, all the iterations in a period (or a quasiperiod) contribute to build-up the growth (and decrease) of the localized profile, while only a part of them in model B contribute. On the other hand the interesting phenomena of noise localization and antilocalization are specific to model B.

A last remark is in order. Focusing our attention on the cases where a slow variable is available, we have cast some basic problems aside. In particular we have not analyzed, for $\varepsilon\neq 0$, the energy spectrum of the stop bands (or of the rotation number).

We conclude by emphasizing the richness and variety of propagation features in quasiperiodic mediums. Models A and B are quite different and are themselves different from other ones previously studied in the literature, such as the quasicrystal model of Luch and Petritis[7] (where the eigenstates are neither extended nor localized and apparently exhibit a recurrent behavior). Last but not least, the resonance phenomena we have described suggest experimental applications: high-resolution frequency filters and small phase shifts detectors.

An experiment on the propagation of acoustic surface waves on a grooved array is presently being performed at Sophia-Antipolis (Thomson-Sintra laboratories), whose preliminary results seem in remarkable agreement with the present theory.[2]

ACKNOWLEDGMENTS

We are indebted to D. Sornette and L. Macon for directing our attention to localization problems, and we

thank them for valuable discussions and insights on the experiments during the course of this work.

APPENDIX A

Lemma 1

In model A, the orbits of the two $\mathring{A}_M$ eigenvectors are symmetrical with respect to the period's center.

Proof. Let $\mathbf{u}_1$ and $\mathbf{u}_2$ be the two eigenvectors of $\mathring{A}_M$, with $\mathbf{u}_i=(u_i^+,u_i^-)$, and Λ_1, Λ_2 be the orbits of $\mathbf{u}_1$ and $\mathbf{u}_2$. Consider now the backward propagation from the right end of the system, of initial state $\mathbf{u}_1^t$ ($\mathbf{u}_1^t$ being the transpose of $\mathbf{u}_1$). Due to the symmetry of the refractive-index field, this state is obviously an eigenstate of $\mathring{A}_M$ and its orbit is symmetric with Λ_1 with respect to the period's center. Since there are only two eigenvectors, Λ_1 and Λ_2 are identical.

Lemma 2

In a pass band, the orbits of the two eigenvectors Λ_1 and Λ_2 are such that $\|\Lambda_1\|(x)=\|\Lambda_1\|(L-x)$ $(i=1,2)$.

Proof. At first eigenvectors $\mathbf{u}_1$ and $\mathbf{u}_2$ associated with eigenvalues s_1 and s_2 verify $\mathbf{u}_1^t=\mathbf{u}_2^*$. Indeed this relation results from $s_2=s_1^*$ and from the characteristic equation of $\mathring{A}_M$. By induction one shows that the elements of Λ_1 and Λ_2 also verify this relation.

Let $\lambda_1^{(n)}=(x_n,y_n)$ be the nth component of Λ_1. We have

$$\|\lambda_1^{(n)}\|^2=(x_n^*,y_n^*)^t(\mathring{A}_n^*)^t\mathring{A}_n(x_n,y_n)\ ,$$

which reads

$$\|\lambda_1^{(n)}\|^2=(|x_n|^2+|y_n|^2)(|a_n|^2+|b_n|^2)$$
$$+x_n^*y_nb_n(a_n+a_n^*)+x_ny_n^*a_n(b_n+b_n^*)\ .$$

The expression for $\|\lambda_2^{(n)}\|^2$ being obtained by making $x_n\rightarrow y_n^*$ and $y_n\rightarrow x_n^*$ in the above expression, one sees that $\|\lambda_1^{(n)}\|=\|\lambda_2^{(n)}\|$, $\forall n$. Finally we have from lemma 1 that $\|\Lambda_1\|(x)=\|\Lambda_2\|(L-x)$, which ends the proof.

APPENDIX B

Let $m\in\mathbb{Z}$. We consider the set $\{a,b\}$ of integers satisfying

$$aF_N-bF_{N+1}=m\ . \tag{B1}$$

(a,b) and (a_0,b_0) being two solutions of (B1), we have

$$(a-a_0)F_N-(b-b_0)F_{N+1}=0\ .$$

Since F_N and F_{N+1} are relatively prime numbers, the above relation implies that

$$a=a_0-kF_{N+1}\ , \tag{B2}$$

$$b=b_0-kF_N\ . \tag{B3}$$

Relations (B2) and (B3) give the complete set $\{a,b\}$ provided we know a particular solution (a_0,b_0). This one can be obtained from a previous relation giving the width of one of the two fundamental pass bands: $F_N^2-F_{N-1}F_{N+1}=(-1)^N$. This relation can be put in the form of Eq. (B1) provided we choose

$$a_0=(-1)^{N+\nu}|m|F_N,\quad b_0=(-1)^{N+\nu}|m|F_{N-1}$$

where $\nu=\text{sign}(m)$.

Now, in order to define the boundaries of the mth energy bands, we must choose the smallest values in the set $\{a,b\}$. This is achieved by taking

$$k=\text{Int}(|m|F_N/F_{N+1})\ .$$

If $N+m$ is even, we obtain $a=|m|F_N-kF_{N+1}$ or

$$E/(2\pi)=|m|F_N/F_{N+1}-\text{Int}(|m|F_N/F_{N+1})\ . \tag{B4}$$

If $N+m$ is odd

$$E/(2\pi)=1+\text{Int}(|m|F_N/F_{N+1})-|m|F_N/F_{N+1}\ . \tag{B5}$$

Relations (B4) and (B5) give one of the boundaries of the mth energy bands, the other one being translated by $\pm m/F_{N+1}$. There are two of them, corresponding to the two symmetrical intervals of the $\{x_j\}$ set.

APPENDIX C

We start from expression (51) and (52) for $\mathring{A}_0^n$ coefficients in the main text, n_0 being arbitrary. Passing to the limit of continuous variables, we put

$$\psi(\Delta x)=\int_x^{x+\Delta x}f(x)dx\ ,$$

where $f(x)$ stands for the local f_n. We have $d\psi/dx=f(x)$. The continuous version of matrix $\mathring{A}_0^n$ is

$$\mathring{A}_x^{x+\Delta x}\approx\begin{bmatrix}\alpha(x) & \beta(x)\\ \beta^*(x) & \alpha^*(x)\end{bmatrix}$$

with

$$\alpha(x)=1+i[1+a(x)]\Delta\psi\ ,$$
$$a(x)=\sin(\phi+\lambda)/(\cos\lambda\sin f)-1\ ,$$
$$\beta(x)=b(x)\Delta\psi,\quad b(x)=i\sin\lambda\, e^{-i\lambda}/\sin f\ .$$

We have $\mathbf{Y}(x+\Delta x)=\mathring{A}_x^{x+\Delta x}\mathbf{Y}(x)$. Introducing $W(x)=Y^+/Y^-$, we obtain

$$dW/d\psi=b+2i(1+a)W-b^*W^2\ , \tag{C1}$$

from which we deduce

$$d(WW^*)/d\psi=(b^*W+bW^*)(1-|W|^2)\ .$$

As expected we find that equality $|W|^2=1$ is preserved by Eq. (C1). Therefore we put $W=e^{i\theta}$, and, using variable ϕ instead of ψ, we find that θ obeys the following equation:

$$(a \sin f/2f)d\theta/d\phi = \sin\lambda\cos(\theta+\lambda)+\sin(\phi+\lambda)/\cos\lambda$$

or, making the variable change $\theta\rightarrow\theta+\lambda$, $\phi\rightarrow\phi+\lambda$,

$$(a \sin f/2f)d\theta/d\phi - \sin\lambda\cos\theta = \sin\phi/\cos\lambda \ , \quad \text{(C2)}$$

with

$$f=\arccos(\cos\phi/\cos\lambda) \ . \quad \text{(C3)}$$

[1]J. B. Sokoloff, Phys. Rep. **126**, 189 (1985).
[2]L. Macon and D. Sornette (unpublished).
[3]J. Belissard, A. Formoso, R. Lima, and D. Testard, Phys. Rev. **26**, 3020 (1982).
[4]S. Aubry and C. André, Proc. Israel Phys. Soc. **3**, 133 (1979).
[5]S. Ostlund and R. Pandit, Phys. Rev. B **29**, 1394 (1984).
[6]F. Delyon and D. Petritis, Commun. Math. Phys. **103**, 441 (1986).
[7]J. M. Luck and D. Petritis, J. Stat. Phys. **42**, 289 (1986).